Transmission phase shift of phonon-assisted tunneling through a quantum dot

Juntao Song,[1] Qing-feng Sun,[1] Hua Jiang,[1] and X. C. Xie[2,1]
[1]*Beijing National Laboratory for Condensed Matter Physics and Institute of Physics, Chinese Academy of Sciences, Beijing 100080, China*
[2]*Department of Physics, Oklahoma State University, Stillwater, Oklahoma 74078, USA*
(Received 15 August 2007; revised manuscript received 21 October 2007; published 9 January 2008)

The influence of electron-phonon interaction on the transmission phase shift of an electron passing through a quantum dot is investigated by using scattering theory. The transmission phase versus the intradot level shows a series of phonon-induced dips. These dips are highly sensitive to the electron-phonon interaction strength λ, and they are much more pronounced than phonon-assisted subpeaks appearing in the conductance. Phonon-induced dephasing is also studied, and the results show that the dephasing probability T_d monotonically increases with the electron-phonon interaction strength λ. The dephasing probability $T_d \propto \lambda^2$ for small λ but $T_d \propto \lambda$ at large λ.

DOI: 10.1103/PhysRevB.77.035309 PACS number(s): 73.63.Kv, 71.38.−k, 03.65.Vf, 03.65.Nk

I. INTRODUCTION

Electron transport through a mesoscopic system, e.g., a quantum dot (QD), has been extensively investigated in the last two decades. Because the size of a mesoscopic device is within the phase coherence length, the phase of the wave function plays a key role in the electronic transport. So the transmission amplitude $t=|t|e^{i\theta}$, which describes the electron tunneling through a mesoscopic system, is a complex number. Its magnitude squared $|t|^2$ is the transmission probability that is observable in measurements of current or conductance. The transmission phase θ describes the phase change when an electron tunnels through a device. This phase θ is in general lost in measurements of current or conductance, so that it is difficult to acquire θ in a general experimental measurement. Using an Aharonov-Bohm (AB) interference ring device, Yacoby *et al.*[1] tried for the first time to measure the transmission phase θ through a QD. Two years later, Schuster *et al.*[2] utilized an open multiterminal AB ring device to successfully measure the phase θ. Since then, investigation of the transmission phase has generated a great deal of theoretical and experimental interest with a fair amount of effort focusing on this field. On the experimental side, for example, Buks *et al.*[3] reported that controlled decoherence could be achieved in a device with a QD that is capacitively coupled to a quantum point contact in its close vicinity. The phase evolution in the Kondo regime was experimentally investigated a few years back,[4,5] and was found to be highly sensitive to the onset of Kondo correlation. Recently, Leturcq *et al.*[6] investigated the magnetic field symmetry and the phase rigidity of the nonlinear conductance in an AB ring. On the other hand, the success of these experiments has generated a number of theoretical studies. In the 1980s, Buttiker found the phase rigidity in a two-terminal AB ring device due to the time-reversal symmetry and the current conservation.[7] After the experiment by Schuster *et al.*,[2] many follow-up theoretical efforts focused on and tried to interpret the measured results of the transmission phase θ through a QD, in particular, the abrupt lapses of θ between two adjacent resonances and the similar behavior of θ for all resonant peaks.[8,9] In addition, some works have also studied the transmission phase in the Kondo regime,[5] or with a photon-assisted tunneling process under a time-dependent external field,[10] etc.

Another subject, the electron-phonon (*e*-ph) interaction in a single-molecule QD, has also generated a great deal of interest in recent years. Phonon-assisted tunneling peaks or steps have been experimentally observed in various single-molecule transistor systems.[11–13] Park *et al.*[11] observed phonon-assisted tunneling substeps in the *I-V* curves in a single-C_{60} transistor device, and those substeps were attributed to the coupling of electrons and the C_{60} surface vibration mode. In another experiment by LeRoy *et al.*,[12] the current and the conductance of a suspended individual single-wall nanotube device were measured, and the phonon-assisted subpeaks on the two sides of the main resonance peak are clearly visible in the differential conductance versus gate voltage, because of the radial breathing phonon mode. On the theoretical side, the influence of the *e*-ph interaction on the mesoscopic transport has also been studied by several groups.[14–16] Many interesting results, e.g., the phonon-assisted subpeaks, etc., were first theoretically predicted, and then experimentally observed.

In this paper, we investigate the transport behavior of a molecular QD system having an *e*-ph interaction by using the scattering matrix method. We focus mainly on the transmission phase of the phonon-assisted tunneling subpeaks, as well as the phonon-induced dephasing process. The results show that the transmission phase θ drops between two adjacent (sub)peaks and θ rises again near the positions of the subpeaks. In particular, the characteristic of phonon-assisted tunneling in the transmission phase is much more pronounced and visible than these subpeaks in the conductance. Afterward, we discuss the dephasing ratio. At zero temperature and at low bias V ($V<\omega_0$ with ω_0 being the phonon frequency), the electronic transport through the molecular QD is completely coherent because the electron cannot absorb or emit phonons under these conditions. However, if at nonzero temperature or at a high bias ($V_{\text{bias}}>\omega_0$), the dephasing process occurs. In the limit of high bias ($V_{\text{bias}}\gg\omega_0$), the dephasing ratio varies as the square of the *e*-ph interaction strength λ in the weak interaction region, but

it is linearly dependent on λ in the strong interaction region. In addition, we also consider an open AB ring device with a molecular QD embedded in one of its arms, and find that it is feasible to experimentally measure the influence of the *e*-ph interaction through the transmission phase.

The rest of this paper is organized as follows. We introduce the model and derive the formula of transmission amplitude in Sec. II. In Sec. III, we present the numerical results and their discussions. In Sec. IV, we study the phase measurement by using an open AB ring device. Finally, a brief summary is presented in Sec. IV. A detailed derivation of the transmission amplitude is given in the Appendix.

II. MODEL AND FORMULATION

The system under consideration is a molecular QD coupled to left and right leads in the presence of a local phonon mode, and it can be described by the following Hamiltonian:

$$H = H_0 + H_1, \tag{1}$$

where

$$H_0 = \sum_{\alpha,k} \varepsilon_{\alpha k} c_{\alpha k}^{\dagger} c_{\alpha k} + \varepsilon_0 d^{\dagger} d + \omega_0 b^{\dagger} b, \tag{2}$$

$$H_1 = \lambda (b^{\dagger} + b) d^{\dagger} d + \sum_{\alpha,k} (t_{\alpha k} c_{\alpha k}^{\dagger} d + \text{H.c.}). \tag{3}$$

Here $c_{\alpha k}^{\dagger}$ ($c_{\alpha k}$) and $d^{\dagger}$ (d) are the electron creation (annihilation) operators in the lead $\alpha = L, R$ and the QD, respectively. $b^{\dagger}$ (b) is the phonon creation (annihilation) operator in the QD. Due to the large level spacing of the molecular QD, only one relevant quantum level ε_0 is considered. The electron in the QD is coupled to a single phonon mode ω_0, and λ and $t_{\alpha k}$ describe the strength of the *e*-ph interaction and the coupling between the QD and the leads, respectively.

In the following, we apply the *S*-matrix scattering formalism to derive the transmission amplitude, the transmission phase, and the current. From Hamiltonian (1), the *S* matrix can be written as[16,17]

$$\begin{aligned} S = 1 &- i \int_{-\infty}^{\infty} dt_1 e^{iH_0 t_1} H_1 e^{-iH_0 t_1} e^{-\eta |t_1|} \\ &- i \int_{-\infty}^{\infty} \int_{-\infty}^{\infty} dt_1 dt_2 e^{iH_0 t_2} H_1 \hat{G}_r(t_2 - t_1) \\ &\times H_1 e^{-iH_0 t_1} e^{-\eta(|t_1| + |t_2|)}, \quad \eta \to 0^+, \end{aligned} \tag{4}$$

where the single-particle Green's function operator $\hat{G}_r(t)$ is $\hat{G}_r(t) = -i\theta(t) e^{-iHt}$. By using the *S* matrix, the final state $|f\rangle$ can be obtained from the initial state $|i\rangle$, with $|f\rangle = S \times |i\rangle$. Considering an initial state $|i\rangle = |\varepsilon_i, n, L\rangle$, which denotes an electron with energy ε_i in the left lead and n phonons in the QD, the final state $|f\rangle$ can be expressed as

$$\begin{aligned} |f\rangle &= S \times |i\rangle = S \times |\varepsilon_i, n, L\rangle \\ &= \sum_{m=-\infty}^{+\infty} [r_m(\varepsilon_f, \varepsilon_i) |\varepsilon_f, m, L\rangle + t_m(\varepsilon_f, \varepsilon_i) |\varepsilon_f, m, R\rangle] \\ &= \sum_{m=-\infty}^{+\infty} [r_m(\varepsilon_i) \delta(\varepsilon_i + n\omega_0 - \varepsilon_f - m\omega_0) |\varepsilon_f, m, L\rangle \\ &\quad + t_m(\varepsilon_i) \delta(\varepsilon_i + n\omega_0 - \varepsilon_f - m\omega_0) |\varepsilon_f, m, R\rangle], \end{aligned} \tag{5}$$

where $t_m(\varepsilon)$ and $r_m(\varepsilon)$ are the transmission amplitude and the reflection amplitude with accompanying absorption or emission of $|m-n|$ phonons. At zero temperature, the phonon number n in the initial state $|i\rangle$ must be zero and then $t_m(\varepsilon_i)$ can be written as (the detailed derivation is shown in the Appendix)

$$\begin{aligned} t_m(\varepsilon_i) &= \int d\varepsilon_f \, t_m(\varepsilon_f, \varepsilon_i) \\ &= -\frac{i}{\sqrt{m!}} \Gamma e^{-\lambda^2} \sum_{l=0}^{m} \frac{(-1)^{m-l} m!}{l!\,(m-l)!} \\ &\quad \times \sum_{n=0}^{\infty} \frac{\lambda^{2n+m}}{n!} \bar{G}^r(\varepsilon_i - n\omega_0 - l\omega_0). \end{aligned} \tag{6}$$

Obviously, $t_0(\varepsilon)$ describes the amplitude of an elastic tunneling process which is coherent, while $t_m(\varepsilon)$ ($m \neq 0$) is the amplitude of an inelastic tunneling process for emitting m phonons. Due to emission of phonons, thus leaving a trace in the QD for the inelastic tunneling process, an inelastically tunneled electron loses its phase coherence. So at zero temperature the transmission phase shift through the QD is[2,9]

$$\theta = \arg\{t_0(0)\}. \tag{7}$$

From $t_m(\varepsilon)$, the total transmission probability (including the coherent and the noncoherent parts) through the QD is $T_{\text{tot}}(\varepsilon) = \Sigma_{m=0}^{\infty} |t_m(\varepsilon)|^2$, and the transmission probability of the noncoherent part is $T_d(\varepsilon) = \Sigma_{m=1}^{\infty} |t_m(\varepsilon)|^2$.

III. NUMERICAL RESULTS AND DISCUSSION

In this section, we numerically study the transmission phase θ and the dephasing ratio T_d/T_{tot}. In our numerical calculations, the phonon frequency ω_0 is set as the energy unity ($\omega_0 = 1$). Notice that the main result of this paper, Eq. (6), is obtained at zero temperature, and thus so are the numerical results and their discussion. However, results at low temperature should be similar to that at zero temperature. Figure 1 shows the coherence transmission probability $|t_0|^2$ [namely, $|t_0(0)|^2$] and the phase θ, as a function of renormalized level $\bar{\varepsilon}_0$, which can be tuned by the gate voltage in an experiment. Notice that $|t_0|^2$ is proportional to the linear conductance G through the QD, $G = (e^2/h)|t_0|^2$. Due to the *e*-ph interaction, several interesting features are manifested. In addition to the main peak related to the single level, new satellite subpeaks appear in the curve of $|t_0|^2 - \bar{\varepsilon}_0$ at $-\bar{\varepsilon}_0 = n\omega_0$ ($n = 1, 2, \ldots$). The subpeaks exist only on the right-hand side of the main peak, and their heights increase with increase of

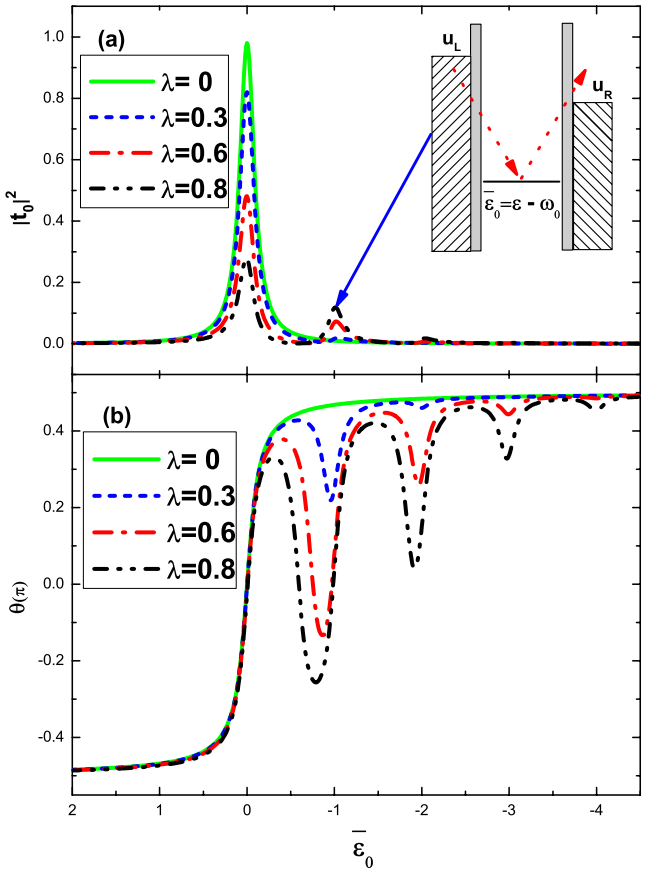

FIG. 1. (Color online) Transmission probability $|t_0|^2$ (a) and transmission phase θ (b) vs the renormalized level $\bar{\varepsilon}_0$ for the different e-ph interaction strengths λ with $\Gamma=0.1$. The inset in (a) is the schematic diagram for the phonon-assisted tunneling process.

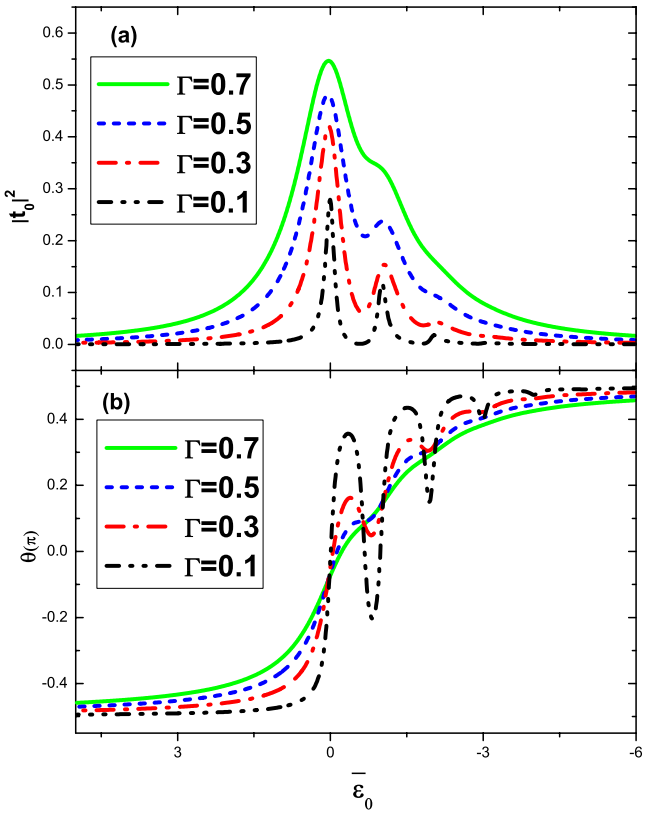

FIG. 2. (Color online) Transmission probability $|t_0|^2$ (a) and transmission phase θ (b) vs the renormalized level $\bar{\varepsilon}_0$ for different Γ with the e-ph interaction strength $\lambda=0.7$.

the e-ph coupling strength λ. The subpeak at $\bar{\varepsilon}_0=-\omega_0$ corresponds to the phonon-assisted tunneling process as shown in the inset of Fig. 1(a), in which an incident electron from the left lead first emits a phonon and tunnels to the level $\bar{\varepsilon}_0$, and subsequently reabsorbs a phonon and tunnels forward to the right lead. Since this process does not leave a trace in the QD, it maintains the phase coherence. Meanwhile, at zero temperature, there is no phonon in the QD in the initial state and the absorption process cannot occur, so that the satellite subpeaks exist only on the negative $\bar{\varepsilon}_0$ side [see Fig. 1(a)].

Next, we study the transmission phase θ which exhibits a nonmonotonic behavior. Across the main resonance peak, θ continuously rises by a value of π. This result is consistent with the previous theoretical and experimental findings.[2,8,9] Because of the e-ph interaction, θ drops between the main peak and the next subpeak or between two adjacent subpeaks, and rises again across a subpeak, such that a dip appears around $-\bar{\varepsilon}_0=n\omega_0$. These dips are much more pronounced than the subpeaks in the transmission probability $|t_0|^2$. For example, for $\lambda=0.8$ the second phonon-assisted subpeak is so small that it is hardly visible [see Fig. 1(a)]; however, even the fourth dip can be clearly seen [see Fig. 1(b)]. The sensitivity of the transmission phase θ to the e-ph interaction provides an additional way to detect the strength of the e-ph interaction.

In the calculations above, the tunneling coupling strength Γ ($\Gamma=\Gamma_L=\Gamma_R$) between the leads and the QD is set to be quite weak, $\Gamma=0.1\ll\omega_0$. With an increase of Γ, the phonon-assisted subpeaks and the main peak in the curve of $|t_0|^2-\bar{\varepsilon}_0$ gradually merge together and become indistinguishable, and the dips in the curve of $\theta-\bar{\varepsilon}_0$ are also gradually getting smaller (see Fig. 2). When $\Gamma\approx\omega_0$ (e.g., $\Gamma=0.7$), all subpeaks and all dips are almost invisible. Consequently, in order to experimentally detect the phonon-induced dips of the phase θ or the phonon-assisted subpeaks, the coupling strength Γ should be tuned to be less than $\omega_0/2$. In fact, the condition $\Gamma<\omega_0/2$ is normally satisfied in experiments.[12]

Let us study the amplitude $t_m(\varepsilon)$ ($m=1,2,\ldots$) of the inelastic tunneling process. In this inelastic tunneling process, an incident electron emits m phonons while tunneling through the QD. However, it is prohibited when $V_{\text{bias}}<m\omega_0$. In the small bias case $V_{\text{bias}}<\omega_0$ and at zero temperature, all inelastic tunneling processes are prohibited and the tunneling through the QD is coherent. On the other hand, with $V_{\text{bias}}>\omega_0$, inelastic tunneling processes occur and the tunneling through the QD is partly noncoherent. In the limit of larger bias voltage, $V_{\text{bias}}\gg\omega_0$, the total dephasing transmission probability $T_d(\varepsilon)$ is $T_d(\varepsilon)=\Sigma_{m=1}^{\infty}|t_m|^2$. Figure 3 shows the dephasing transmission probability T_d (or T_d/T_{tot}) versus renormalized level $\bar{\varepsilon}_0$ and the e-ph interaction strength λ, while, without the e-ph interaction (namely, $\lambda=0$), no inelastic tunneling process happens and thus $T_d=0$. When $\lambda\neq0$, the inelastic tunneling process occurs and T_d is

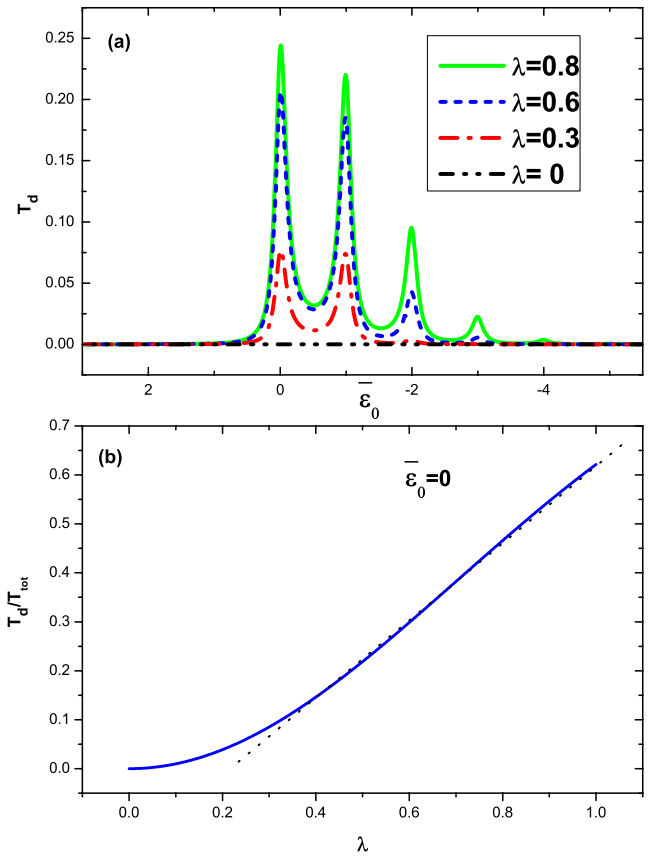

FIG. 3. (Color online) (a) e-ph coupling strength λ dependence of the dephasing probability T_d. (b) Relative dephasing probability $T_d/T_{\rm tot}$ vs λ. The parameter $\Gamma=0.1$ in (a) and (b). The dotted line in (b) is a guide to the eye.

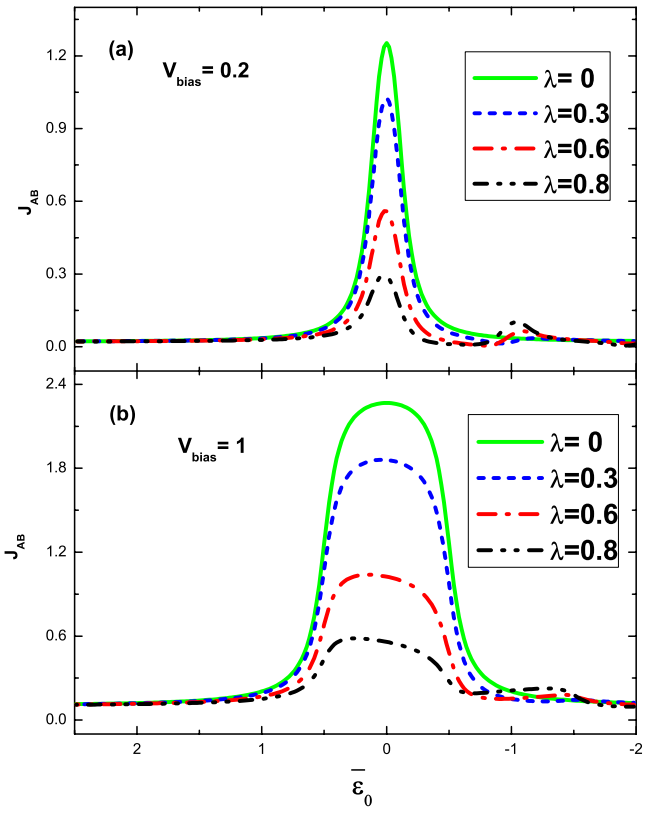

FIG. 4. (Color online) Current $J_{\rm AB}$ vs the renormalized level $\bar{\varepsilon}_0$ for different e-ph interaction strengths λ with $\Gamma=0.1$, $\phi=0$, and $t_{\rm ref}=0.1$.

no longer zero. A series of peaks are exhibited in the curve of $T_d-\bar{\varepsilon}_0$ and the interval between the two adjacent peaks is ω_0 [see Fig. 3(a)]. As is seen from Fig. 3(a), a higher peak must correspond to a larger value of λ (including the peak at $\bar{\varepsilon}_0=0$). This means that the dephasing probability T_d monotonically increases with λ, regardless of the position of the renormalized level $\bar{\varepsilon}_0$. Next, in Fig. 3(b) we show the relative dephasing transmission probability T_d/T_{tot} versus the e-ph coupling strength λ in the resonant tunneling region (namely, $\bar{\varepsilon}_0=0$). When λ is small ($\lambda<0.2\omega_0$), the relative dephasing transmission probability $T_d/T_{\rm tot}$ increases parabolically with λ, but the dephasing probability $T_d/T_{\rm tot}$ is found to increase linearly with increasing λ in the range $1>\lambda>0.4$. For the large λ case ($\lambda>1$), $T_d/T_{\rm tot}>0.6$ and the dephasing inelastic tunneling processes dominate. In an experiment the parameter $g=(\lambda/\omega_0)^2$ is generally in the range from 0.1 to 1,[13] though some special devices[18] show a big variable range of g. In this λ region, the degree of dephasing is linearly dependent on the e-ph coupling strength.

IV. THE AB RING DEVICE

In Secs. II and III, we consider only a simple device consisting of a QD coupled to two leads. However, in a real experiment to measure the transmission phase θ, the device is an open AB ring with a QD embedded in one of the arms.[2] Therefore, it is of experimental relevance to study the open AB ring device in this section. A QD is embedded in one arm of the ring, and the other arm is the reference arm with the transmission amplitude $t_{\rm ref}$. Due to openness of the open AB ring device, the process of circling multiple times around the ring is negligible. Note that only elastic tunneling process $t_0(\varepsilon_i)$ is in interference with the reference arm. $T_{\rm AB}(\varepsilon_f,\varepsilon_i)$, defined as the probability that an electron of energy ε_i incident from the left lead will be transmitted with energy ε_f into the right lead, can therefore be written as

$$T_{\rm AB}(\varepsilon_f,\varepsilon_i)=\sum_{m=0}^{\infty}\delta(\varepsilon_i-\varepsilon_f-m\omega_0)|t_m(\varepsilon_i)+\delta_{m,0}e^{i\phi}t_{\rm ref}|^2, \quad (8)$$

where ϕ is the magnetic flux inside the ring. In the absence of the reference arm (namely, $t_{\rm ref}=0$), $T_{\rm AB}(\varepsilon_f,\varepsilon_i)$ is reduced to $T(\varepsilon_f,\varepsilon_i)=\Sigma_{m=0}^{\infty}\delta(\varepsilon_i-\varepsilon_f-m\omega_0)|t_m(\varepsilon_i)|^2$, and this result is the same as that in the work by Wingreen *et al.*[16] Using the transmission probability $T_{\rm AB}(\varepsilon_f,\varepsilon_i)$, the current flowing through the AB ring is[16]

$$J_{AB}=\frac{2e}{h}\int d\varepsilon_i\int d\varepsilon_f T_{\rm AB}(\varepsilon_f,\varepsilon_i)f_L(\varepsilon_i)[1-f_R(\varepsilon_f)]$$
$$-\frac{2e}{h}\int d\varepsilon_i\int d\varepsilon_f T_{\rm AB}(\varepsilon_f,\varepsilon_i)f_R(\varepsilon_i)[1-f_L(\varepsilon_f)], \quad (9)$$

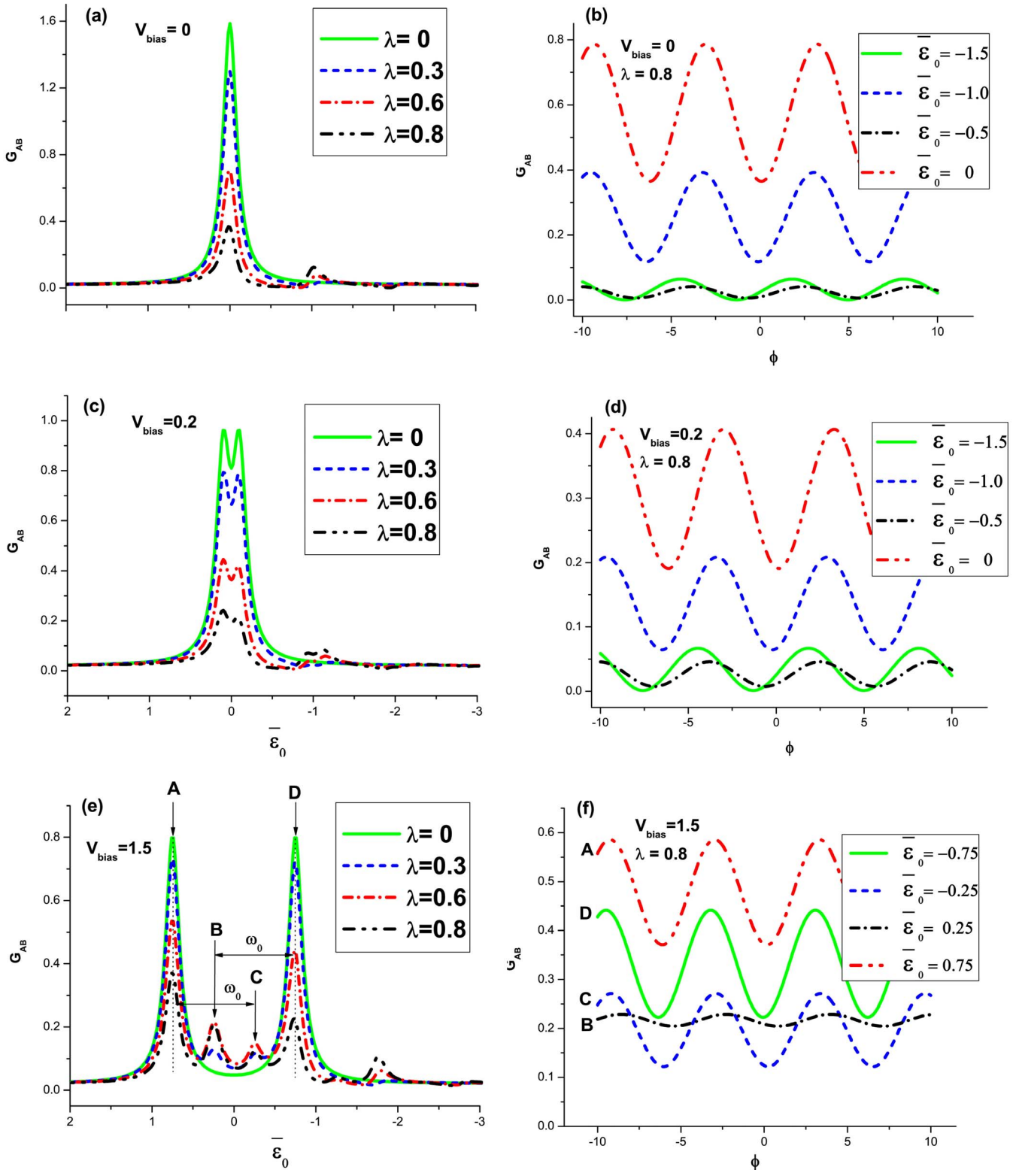

FIG. 5. (Color online) (a),(c),(e) Differential conductance G_{AB} vs the level $\bar{\varepsilon}_0$ for the bias $V_{bias}=0$ (a), 0.2 (c), and 1.5 (e) at $\phi=0$. (b),(d),(f) Differential conductance G_{AB} vs the magnetic flux ϕ for the bias $V_{bias}=0$ (b), 0.2 (d), and 1.5 (f). The other parameters are $\Gamma=0.1$ and $t_{ref}=0.1$.

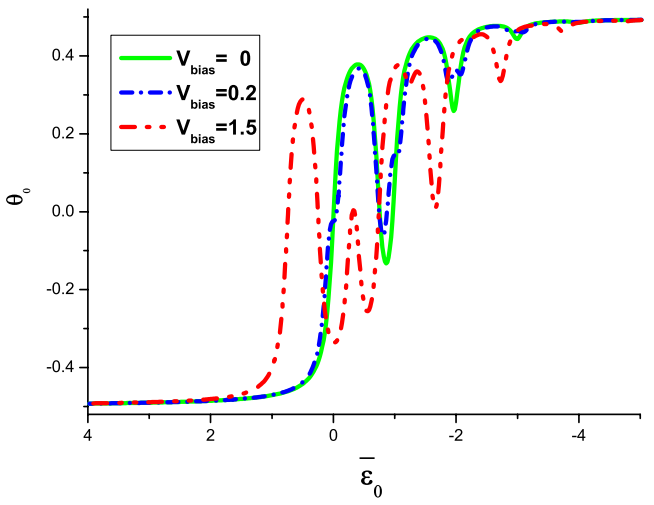

FIG. 6. (Color online) Phase θ_0 vs the level $\bar{\varepsilon}_0$ for the different bias V_{bias}. The other parameters are $\lambda=0.6$, $\Gamma=0.1$, and $t_{\text{ref}}=0.1$.

where $f_L(\varepsilon_i)=f(\varepsilon_i-\mu_L)$ and $f_R(\varepsilon_f)=f(\varepsilon_f-\mu_R)$ with the chemical potential $\mu_{L(R)}=\pm eV_{\text{bias}}/2$, and $f(\varepsilon)$ is the Fermi distribution function. Finally, the differential conductance G_{AB} can be obtained from $G_{\text{AB}}=dJ_{\text{AB}}/dV_{\text{bias}}$.

Based on Eq. (9), we show the numerical results for the current J_{AB} flowing through the open AB ring in Fig. 4. Figures 4(a) and 4(b) correspond to the small and large bias voltage cases, respectively. In both cases, phonon-assisted subpeaks can be seen on the right-hand side of the main peak, and the subpeak height increases with increasing e-ph coupling strength λ. These results for the current are similar to those in a previous paper.[16]

Next, we focus on the differential conductance G_{AB} ($G_{\text{AB}}=dJ_{\text{AB}}/dV_{\text{bias}}$) and its dependence on the renormalized level $\bar{\varepsilon}_0$ or on the magnetic flux ϕ. In fact, $\bar{\varepsilon}_0$ and ϕ can be well controlled and are continuously tunable in an experiment. The differential conductance G_{AB} is always a periodic function of the magnetic flux ϕ with a period of 2π. Figures 5(a) and 5(b) show the linear conductance G_{AB} at zero bias voltage. Here a series of phonon-assisted subpeaks is exhibited in the curve of G_{AB} versus $\bar{\varepsilon}_0$, similar to that in the transmission probability $|t_0|^2$ [see Fig. 1(a)] because of the small value of t_{ref}. In addition, the phonon-assisted tunneling processes can also be observed from the amplitude of the G_{AB} oscillation versus the magnetic flux ϕ [see Fig. 5(b)]. When $\bar{\varepsilon}_0=0$ or -1 (i.e., at the main peak or the first subpeak), the AB oscillation amplitudes are quite large since the phonon-assisted elastic tunneling processes play a role here. But at the position between two adjacent peaks (e.g., $\bar{\varepsilon}_0=-0.5$ or -1.5), the AB oscillation amplitude is quite weak. When a small bias voltage is applied between the left and right leads, all peaks in the curve of $G_{\text{AB}}-\bar{\varepsilon}_0$, including the main peak and phonon-assisted subpeaks, split into two [see Fig. 5(c)], and their positions are at $\bar{\varepsilon}_0=m\omega_0\pm V_{\text{bias}}/2$. The reason is that, at these values of $\bar{\varepsilon}_0=m\omega_0\pm V_{\text{bias}}/2$, the renormalized level $\bar{\varepsilon}_0$ is in line with the left or the right chemical potential $\mu_{L,R}=\pm V_{\text{bias}}/2$, or the distance between $\bar{\varepsilon}_0$ and $\mu_{L,R}$ is just $m\omega_0$. The behavior of the conductance G_{AB} versus the magnetic flux ϕ for small bias is similar to that of the linear conductance [see Figs. 5(b) and 5(d)]. Note that at zero or small bias ($V_{\text{bias}}<\omega_0$) all tunnelings through the QD are completely coherent, and the small amplitude oscillation in G_{AB} is due to the small transmission probability $|t_0|^2$. Finally, we investigate the large bias case ($V_{\text{bias}}>\omega_0$). At large bias the peaks in the curve of G_{AB} versus $\bar{\varepsilon}_0$ clearly split into two with an interval of V_{bias}. Moreover, some extra subpeaks emerge even on the left of the main peak. For example, the subpeak marked by B in Fig. 5(e) stands on the left of the main peak at $\bar{\varepsilon}_0=-V_{\text{bias}}/2$, and their interval is ω_0. In fact, this peak is from the inelastic tunneling process $t_1(\varepsilon)$ and a phonon is left in the QD with an electron tunneling through the dot. Figure 5(f) shows the conductance G_{AB} versus the magnetic flux ϕ while the level $\bar{\varepsilon}_0$ is fixed on the peak positions of Fig. 5(e). The amplitude of the AB oscillation of the peak B is very weak, but the amplitudes are quite large for other three peaks. This gives a proof that the peak B is indeed from the inelastic tunneling process, and the corresponding tunneling electron loses its phase coherence.

Since the differential conductance G_{AB} is a periodic function of the magnetic flux ϕ, one can make the Fourier expansion $G_{\text{AB}}(\phi)=G^0_{\text{AB}}+G'_{\text{AB}}\cos(\phi+\theta_0)$. Here the initial phase θ_0 is a directly experimentally measurable quantity. Let us compare the measured phase θ_0 with the transmission phase θ. Figure 6 shows the phase θ_0 versus $\bar{\varepsilon}_0$ for different bias V_{bias}. At zero bias voltage the characteristics of the phase θ_0, including the phonon-induced dips, are completely the same as for the transmission phase θ (see Fig. 1). When a small bias voltage (e.g., $V_{\text{bias}}=0.2<\omega_0$) is applied between the two leads, the phase θ_0 changes slightly but can still reflect the transmission phase θ quantitatively. So at zero or small bias the transmission phase θ, including the intriguing characteristics due to the e-ph interaction, can be directly observed through the measurement of the differential conductance versus the intradot level. For a molecular QD device, the phonon frequency ω_0 is usually from 5 to 35 meV,[11,12] so the condition $V_{\text{bias}}<\omega_0$ is easily reachable. On the other hand, at large bias (e.g., $V_{\text{bias}}=1.5\omega_0$), the phase θ_0 deviates substantially from the transmission phase θ.

V. CONCLUSIONS

In summary, we study the influence of the electron-phonon (e-ph) interaction on the transmission phase and the dephasing while electrons tunnel through a molecular quantum dot. It is found that the transmission phase versus the intradot level exhibits a nonmonotonic behavior, and a pronounced dip emerges when the renormalized level is located at the position of the phonon-assisted subpeaks. In particular, phonon-induced dips in the transmission phase are much more apparent than the phonon-assisted subpeaks in the conductance. In addition, phonon-induced dephasing increases monotonically with the e-ph interaction strength λ. The dephasing probability T_d is proportional to λ^2 at small λ, but $T_d\propto\lambda$ for large λ. In addition, an open AB ring device is investigated. At zero or small bias, the measurement phase from the differential conductance versus the magnetic flux is

found to have the same characteristics as the transmission phase, including the phonon-induced dips.

ACKNOWLEDGMENTS

We are grateful to Jianing Zhuang for his helpful discussions. This work is supported by U.S. DOE under Grant No. DE-FG02-04ER46124, NSF under Grant No. CCF-052473, and NSF China under Grants No. 10474125 and No. 10525418.

APPENDIX

In this appendix, we present a detailed derivation of the transmission amplitude $t_m(\varepsilon_i)$, Eq. (6). Because those states are normalized according to $\langle \varepsilon, n, \alpha | \varepsilon', n', \alpha' \rangle = \delta_{n,n'} \delta_{\alpha,\alpha'} \delta(\varepsilon - \varepsilon')$, only the last term in the S matrix [Eq. (4)] contributes to the scattering matrix element $t_m(\varepsilon_f, \varepsilon_i)$.[16] Therefore the scattering matrix element $t_m(\varepsilon_f, \varepsilon_i)$ is reduced to

$$\begin{aligned} t_m(\varepsilon_f, \varepsilon_i) &= \langle \varepsilon_f, m, R | S | \varepsilon_i, 0, L \rangle \\ &= -\int_{-\infty}^{\infty} \int_{-\infty}^{\infty} dt_1 dt_2 \theta(t_2 - t_1) e^{-\eta(|t_1|+|t_2|)} \\ &\quad \times e^{i(\varepsilon_f + m\omega_0)t_2 - i\varepsilon_i t_1} \langle \varepsilon_f, m, R | H_1 e^{-iH(t_2 - t_1)} H_1 | \varepsilon_i, 0, L \rangle. \end{aligned} \tag{A1}$$

Taking the change of variables $t_1 = t_1$ and $t = t_2 - t_1$, the integration over t_1 now yields a δ function of energies as $\eta \to 0^+$, and $t_m(\varepsilon_f, \varepsilon_i)$ changes to

$$\begin{aligned} t_m(\varepsilon_f, \varepsilon_i) &= \langle \varepsilon_f, m, R | S | \varepsilon_i, 0, L \rangle = -2\pi\delta(\varepsilon_i - \varepsilon_f - m\omega_0) \int_{-\infty}^{\infty} dt\ \theta(t) e^{i\varepsilon_i t} \times \langle \varepsilon_f, m, R | H_1 e^{-iHt} H_1 | \varepsilon_i, 0, L \rangle \\ &= -2\pi\delta(\varepsilon_i - \varepsilon_f - m\omega_0) \int_{-\infty}^{\infty} dt\ \theta(t) e^{i\varepsilon_i t} \sum_{k'} \sum_{k} t_{Rk'} t_{Lk}^* \langle \varepsilon_f, m, R | c_{Rk'}^\dagger d e^{-iHt} d^\dagger c_{Lk} | \varepsilon_i, 0, L \rangle \\ &= -2\pi\delta(\varepsilon_i - \varepsilon_f - m\omega_0) \int_{-\infty}^{\infty} dt\ \theta(t) e^{i\varepsilon_i t} \times t_R(\varepsilon_f) t_L^*(\varepsilon_i) \langle m | d e^{-iHt} d^\dagger | 0 \rangle \\ &= -2\pi\delta(\varepsilon_i - \varepsilon_f - m\omega_0) \int_{-\infty}^{\infty} dt\ \theta(t) e^{i\varepsilon_i t} \times t_R(\varepsilon_f) t_L^*(\varepsilon_i) \left\langle 0 \left| \frac{b^m}{\sqrt{m!}} d e^{-iHt} d^\dagger \right| 0 \right\rangle \\ &= -2\pi\delta(\varepsilon_i - \varepsilon_f - m\omega_0) \int_{-\infty}^{\infty} dt\ \theta(t) e^{i\varepsilon_i t} \times t_R(\varepsilon_f) t_L^*(\varepsilon_i) \left\langle 0 \left| \frac{b^m(t)}{\sqrt{m!}} d(t) d^\dagger \right| 0 \right\rangle, \end{aligned} \tag{A2}$$

where $|t_{L(R)}(\varepsilon)|^2 = \Sigma_k |t_{Lk(Rk)}|^2 \delta(\varepsilon - \varepsilon_{Lk(Rk)})$.[8,16] At zero temperature, the above equation can be rewritten as

$$\begin{aligned} t_m(\varepsilon_f, \varepsilon_i) &= -2\pi\delta(\varepsilon_i - \varepsilon_f - m\omega_0) \frac{t_R(\varepsilon_f) t_L^*(\varepsilon_i)}{\sqrt{m!}} \\ &\quad \times \int_{-\infty}^{\infty} dt\ \theta(t) e^{i\varepsilon_i t} \mathrm{Tr}[b^m(t) d(t) d^\dagger]. \end{aligned} \tag{A3}$$

In order to calculate $\mathrm{Tr}[b^m(t) d(t) d^\dagger]$, we apply a canonical transformation with[19] $\bar{H} = e^s H e^{-s}$ and $s = (\lambda/\omega_0)(b^\dagger - b) d^\dagger d$,. Under this canonical transformation, Hamiltonian (1) becomes

$$\bar{H} = \bar{H}_{\mathrm{el}} + \bar{H}_{\mathrm{ph}}, \tag{A4}$$

where

$$\bar{H}_{\mathrm{el}} = \sum_{\alpha,k} \varepsilon_{\alpha k} c_{\alpha k}^\dagger c_{\alpha k} + \bar{\varepsilon}_0 d^\dagger d + \sum_{\alpha,k} (\bar{t}_{\alpha k} c_{\alpha k}^\dagger d + \mathrm{H.c.}), \tag{A5}$$

$$\bar{H}_{\mathrm{ph}} = \omega_0 b^\dagger b, \tag{A6}$$

where $\bar{\varepsilon}_0 = \varepsilon_0 - g\omega_0$ is the renormalized level of the QD and $\bar{t}_{\alpha k} = t_{\alpha k} X$, with $g \equiv (\lambda/\omega_0)^2$ and $X \equiv \exp[-(\lambda/\omega_0)(b^\dagger + b)]$. Next we employ the same approximation as the one in Ref. 15, $\bar{t}_{\alpha k} \approx t_{\alpha k}$. Under this approximation, the e-ph interaction can be decoupled and $t_m(\varepsilon_f, \varepsilon_i)$ in Eq. (A3) becomes

$$\begin{aligned} t_m(\varepsilon_f, \varepsilon_i) &= -2\pi\delta(\varepsilon_i - \varepsilon_f - m\omega_0) \frac{t_R(\varepsilon_f) t_L^*(\varepsilon_i)}{\sqrt{m!}} \\ &\quad \times \int_{-\infty}^{\infty} dt\ \theta(t) e^{i\varepsilon_i t} \mathrm{Tr}[b^m(t) \bar{d}(t) X(t) \bar{d}^\dagger X^\dagger] \\ &= -i2\pi\delta(\varepsilon_i - \varepsilon_f - m\omega_0) \frac{t_R(\varepsilon_f) t_L^*(\varepsilon_i)}{\sqrt{m!}} \\ &\quad \times \int_{-\infty}^{\infty} dt\ e^{i\varepsilon_i t} \bar{G}^r(t) e^{-\Phi_m(t)}, \end{aligned} \tag{A7}$$

where $\bar{G}^r(t)=-i\theta(t)\mathrm{Tr}_{\mathrm{el}}[\bar{d}(t)\bar{d}^\dagger]=-i\theta(t)\langle 0|\bar{d}(t)\bar{d}^\dagger|0\rangle$ and $e^{-\Phi_m(t)}=\mathrm{Tr}_{\mathrm{ph}}[b^m(t)X(t)X^\dagger]$. Using the method of Feynman disentangling of operators,[19] $e^{-\Phi_m(t)}$ can be obtained:

$$\begin{aligned} e^{-\Phi_m(t)} &= \mathrm{Tr}_{\mathrm{ph}}[b^m(t)X(t)X^\dagger] = \langle 0|b^m(t)X(t)X^\dagger|0\rangle_{\mathrm{ph}} \\ &= e^{-\lambda u}\langle 0|b^m(t)e^{b^\dagger u^*}e^{-bu}|0\rangle_{\mathrm{ph}} \\ &= e^{-\lambda u}e^{-im\omega_0 t}\langle 0|b^m e^{b^\dagger u^*}|0\rangle_{\mathrm{ph}} \\ &= e^{-\lambda u}e^{-im\omega_0 t}\frac{(u^*)^m}{m!}\langle 0|b^m(b^\dagger)^m|0\rangle_{\mathrm{ph}} = e^{-\lambda u}e^{-im\omega_0 t}(u^*)^m, \end{aligned} \tag{A8}$$

where $u=\lambda(1-e^{-i\omega_0 t})$. Substituting Eq. (A8) into Eq. (A7), we have

$$\begin{aligned} t_m(\varepsilon_f,\varepsilon_i) &= -i2\pi\delta(\varepsilon_i-\varepsilon_f-m\omega_0)\frac{t_R(\varepsilon_f)t_L^*(\varepsilon_i)}{\sqrt{m!}} \\ &\times\int_{-\infty}^{\infty} dt\, e^{i\varepsilon_i t}\bar{G}^r(t)e^{-\lambda u}e^{-im\omega_0 t}(u^*)^m \\ &= -\frac{i}{\sqrt{m!}}\Gamma e^{-\lambda^2}\sum_{l=0}^{m}\frac{(-1)^{m-l}m!}{l!\,(m-l)!} \\ &\times\sum_{n=0}^{\infty}\frac{\lambda^{2n+m}}{n!}\bar{G}^r(\varepsilon_i-n\omega_0-l\omega_0), \end{aligned} \tag{A9}$$

where $\bar{G}^r(E)$ is the Fourier transform of $\bar{G}^r(t)$. Here we have assumed symmetric coupling [$t_L(\varepsilon_i)=t_R(\varepsilon_i)$] and considered the wideband limit case, so $\Gamma=2\pi t_{L(R)}(\varepsilon_f)t_{L(R)}^*(\varepsilon_i)$ is independent of the energy ε_i and ε_f. In the wideband limit the Green's function $\bar{G}^r(\varepsilon)$ is easily calculated following the standard procedure,[15,20,21]

$$\bar{G}^r(\varepsilon)=\frac{1}{\varepsilon-\bar{\varepsilon}_0+i\Gamma}. \tag{A10}$$

From $t_m(\varepsilon_f,\varepsilon_i)$, the transmission amplitude $t_m(\varepsilon_i)$ can be obtained: $t_m(\varepsilon_i)=\int d\varepsilon_f t_m(\varepsilon_f,\varepsilon_i)$, and the result is given in Eq. (6) in the text.

[1] A. Yacoby, M. Heiblum, D. Mahalu, and H. Shtrikman, Phys. Rev. Lett. **74**, 4047 (1995).

[2] R. Schuster, E. Buks, M. Heiblum, D. Mahalu, V. Umansky, and H. Shtrikman, Nature (London) **385**, 417 (1997).

[3] E. Buks, R. Schuster, M. Heiblum, D. Mahalu, and V. Umansky, Nature (London) **391**, 871 (1998).

[4] Yang Ji, M. Heiblum, D. Sprinzak, D. Mahalu, and Hadas Shtrikman, Science **290**, 779 (2000); Yang Ji, M. Heiblum, and Hadas Shtrikman, Phys. Rev. Lett. **88**, 076601 (2002).

[5] Ulrich Gerland, Jan von Delft, T. A. Costi, and Yuval Oreg, Phys. Rev. Lett. **84**, 3710 (2000).

[6] R. Leturcq, D. Sanchez, G. Gotz, T. Ihn, K. Ensslin, D. C. Driscoll, and A. C. Gossard, Phys. Rev. Lett. **96**, 126801 (2006).

[7] M. Büttiker, Phys. Rev. Lett. **57**, 1761 (1986).

[8] A. L. Yeyati and M. Buttiker, Phys. Rev. B **52**, R14360 (1995); G. Hackenbroich and H. A. Weidenmüller, Phys. Rev. Lett. **76**, 110 (1996); Phys. Rev. B **53**, 16379 (1996); Q. Sun and T. Lin, Eur. Phys. J. B **5**, 913 (1998); Q.-F. Sun and T.-H. Lin, J. Phys.: Condens. Matter **10**, 3581 (1998).

[9] G. Hackenbroich, Phys. Rep. **343**, 463 (2001).

[10] Q.-F. Sun, J. Wang, and T.-H. Lin, Phys. Rev. B **60**, R13981 (1999).

[11] H. Park, J. Park, A. K. L. Lim, E. H. Anderson, A. P. Alivisatos, and P. L. McEuen, Nature (London) **407**, 57 (2000).

[12] B. J. LeRoy, S. G. Lemay, J. Kong, and C. Dekker, Nature (London) **432**, 371 (2004); B. J. LeRoy, J. Kong, V. K. Pahilwani, C. Dekker, and S. G. Lemay, Phys. Rev. B **72**, 075413 (2005).

[13] S. Sapmaz, P. Jarillo-Herrero, Y. M. Blanter, C. Dekker, and H. S. J. van der Zant, Phys. Rev. Lett. **96**, 026801 (2006).

[14] David M.-T. Kuo and Y. C. Chang, Phys. Rev. B **66**, 085311 (2002); K. Flensberg, *ibid.* **68**, 205323 (2003); Z. Z. Chen, R. Lu, and B. F. Zhu, *ibid.* **71**, 165324 (2005); J. T. Song, Q.-F. Sun, J. H. Gao, and X. C. Xie, *ibid.* **75**, 195320 (2007).

[15] J. X. Zhu and A. V. Balatsky, Phys. Rev. B **67**, 165326 (2003).

[16] N. S. Wingreen, K. W. Jacobsen, and J. W. Wilkins, Phys. Rev. B **40**, 11834 (1989).

[17] J. R. Taylor, *Scattering Theory* (Plenum, New York, 1981), pp. 269–310.

[18] A. N. Pasupathy, J. Park, C. Chang, A. V. Soldatov, S. Lebedkin, R. C. Bialczak, J. E. Grose, L. A. K. Donev, J. P. Sethna, D. C. Ralph, and P. L. McEuen, Nano Lett. **5**, 203 (2005).

[19] G. D. Mahan, *Many-Particle Physics*, 3rd ed. (Plenum Press, New York, 2000).

[20] A.-P. Jauho, N. S. Wingreen, and Y. Meir, Phys. Rev. B **50**, 5528 (1994).

[21] H. Huag and A.-P. Jauho, in *Quantum Kinetics in Transport and Optics of Semiconductors*, edited by Helmut K. V. Lotsch (Springer-Verlag, Berlin, 1996).